International Journal of Fatigue 90 (2016) 116–124

Contents lists available at ScienceDirect

International Journal of Fatigue

journal homepage: www.elsevier.com/locate/ijfatigue

Frequency effect in short-beam shear fatigue of a glass fiber reinforced polyester composite

Héctor Kotik [a,b,c,*], Juan Perez Ipiña [a]

[a] Grupo Mecánica de Fractura, Universidad Nacional del Comahue/CONICET, Buenos Aires 1400, Neuquén CP 8300, Argentina
[b] Universidad Nacional del Sur, Departamento de ingeniería, Avenida Colón 80, Bahía Blanca 8000FTN, Argentina
[c] IMPSA/CONICET/Grupo Mecánica de Fractura, Buenos Aires 1400, Neuquén CP 8300, Argentina

ARTICLE INFO

Article history:
Received 18 December 2015
Received in revised form 7 April 2016
Accepted 23 April 2016
Available online 26 April 2016

Keywords:
Short-beam shear test
Interlaminar shear fatigue
Frequency
Glass reinforced polyester

ABSTRACT

The effect of loading frequency on short-beam shear fatigue behavior of a glass fiber reinforced polyester laminated was studied. Surface specimen temperature increase and macroscopic specimen damage were also evaluated. The tests were performed employing a short-beam device with three amplitude stress levels, four frequencies between 1 and 10 Hz and a shear stress ratio $R = 0.1$. Specimens with the smallest stress amplitude showed a fatigue life between 10^5 and 10^6 cycles and the largest stress amplitude endured approximately 10^4 cycles. The high stress amplitude tests produced increases in specimen temperature up to 7 °C, 4 °C and 1 °C for 10 Hz, 6 Hz and both 3 and 1 Hz respectively, while no temperature changes were measured in low amplitude tests. According to the statistical analysis performed, the changes in fatigue life were not significant for the frequency range employed in this study.

1. Introduction

Fatigue tests are time-consuming, especially in high cycle fatigue. High loading frequencies are desirable as long as no significant change occurs in the fatigue behavior. Selecting the optimal testing frequency for composite tests is not an easy task because of its frequency sensitivity. There are no clear guidelines, although some directions, as no significant change of specimen temperature, are widely used [1]. Nevertheless, these directions sometimes do not consider influential variables as the principal fiber orientation or the type of fiber and matrix, among others.

The change in fatigue life due to frequency variation has been associated with two effects [2]. The first one is self-generated heating due to the high damping factor and the low heat conductivity of the matrix. The second one is the effect of rate dependence. Nijssen [3] included a third effect, the frictional heating generated between the specimen and the test device. These effects are linked to the specimen geometry, the material system, load direction in the laminate, etc. [1]. For example, when the load is applied in the principal fiber direction, the composite usually is less sensitive to changes in loading frequency than in directions where matrix or fiber–matrix interface control the mechanical behavior. The latter is the case of interlaminar shear properties that are dependent of matrix and fiber–matrix interface behavior.

Interlaminar shear fatigue behavior is of special interest in laminate composites of large thickness (>20 mm) and flexure cyclic loads, as can be found in wind turbine blades. Different tests have been proposed to measure this behavior [4–9], many of which are adaptations of quasi-static tests. Short-beam shear (SBS) test is one of the proposals and it has the advantages of small specimens and simple test device, together to no grip problems. The quasi-static SBS test is widely used to compare materials or in quality control. Although the specimens do not present a pure shear stress state, the stress state promotes the interlaminar failure of the specimens [10]. This test has been used by several researchers [4,11–13] to measure predominant interlaminar shear fatigue of composites and ASTM Committee D30 has been working in its normalization [14]. The selection of a loading frequency in SBS fatigue tests is not simple just as in other fatigue tests in composites. The frequencies employed in fatigue tests of polymer matrix composites are usually below 25 Hz [15]. The public databases of SNL/MSU/DOE [16] and Knowledge Centre WMC [17] were consulted with the aim to know usual frequency values in composite fatigue of glass and carbon reinforced polymers. The histograms of loading frequencies are shown in Figs. 1 and 2. Data correspond to results of specimens tested with different lay-ups, geometries, production processes, fiber/resin ratios and directions of load application with regard to principal fiber direction. Tests were carried out at

* Corresponding author at: Grupo Mecánica de Fractura, Universidad Nacional del Comahue/CONICET, Buenos Aires 1400, Neuquén CP 8300, Argentina.
E-mail address: hector.kotik@fain.uncoma.edu.ar (H. Kotik).

http://dx.doi.org/10.1016/j.ijfatigue.2016.04.025
0142-1123/

Nomenclature

b	specimen width
CLD	constant life diagrams
CV	sample coefficient of variation
E^{chord}	tensile chord modulus of elasticity
f	loading frequency
F^{sbs}	quasi-static short-beam strength
F^{tu}	ultimate tensile strength
h	specimen thickness
l	specimen length
N	number of cycles
N_f	number of cycles at failure or SBS fatigue life of a specimen
P	force
$P_{(i)}$	force at ith data point observed during the fatigue test
R	shear stress-ratio
R^2	coefficient of determination
S	standard deviation
SBS	Short-beam shear
α	significance level
δ	displacement of the loading nose
δmax ratio	stiffness loss of the specimen
$\Delta\delta$ ratio	variation in displacement at each load cycle/variation in displacement at the first cycle ratio
δmax_N	maximum displacement of the loading nose at N cycles
δmax_1	maximum displacement of the loading nose at the first cycle
δmin_N	minimum displacement of the loading nose at N cycles
δmin_1	minimum displacement of loading nose at the first cycle
v	Poisson's ratio
τ_a	shear stress amplitude
$\tau^{sbs}_{(i)}$	SBS stress value observed at ith data point in one cycle
τ^{sbs}_{max}	maximum SBS stress value observed in one cycle
τ^{sbs}_{min}	minimum SBS stress value observed in one cycle

constant amplitude loading, different stress levels and uniaxial tension–tension, tension–compression and compression–compression loads. The associated published papers in both databases [16,17] give more information about the test programs. No interlaminar shear tests are included in the cited databases.

In the case of SNL/MSU/DOE database, the most employed frequencies changed with time: Up to 2006 more than 28% of the tests were performed with values higher than 10.5 Hz. In the following six years, around 0.2% of tests were performed above 10.5 Hz. This change is associated to testing programs with different objectives. Many of the test with frequencies above 10.5 Hz corresponded to very high cycles (10^8–10^9 cycles) testing programs. Moreover, many of these fatigue tests were performed varying the frequency to maintain similar load rate and reduce test time at high cycle fatigue. In the case of Knowledge Centre WMC's database, less than 1% of the tested values were over 10.5 Hz. Van Wingerde et al. [18] discussed these database results and commented that a larger than expected influence of the loading frequency was observed. Frequencies employed in some interlaminar shear fatigue tests are presented in Table 1. Recent papers dealing with high cycle fatigue have used 10 Hz or lower frequencies.

The selection of an optimum or, at least, adequate loading frequency for SBS fatigue test is affected by all the aforementioned aspects. Because of the lack of specific published information, this paper examines the effect of frequencies in the SBS fatigue life of a glass fiber reinforced polyester laminate. The range of frequencies covered values between 1 and 10 Hz, commonly employed in recent fatigue test. A variance analysis was performed to evaluate whether significant changes in fatigue life are present. The macroscopic damage and the temperature change in the specimen surface were also evaluated.

2. Material and methods

The studied material was a glass fiber reinforced polyester laminate. The reinforcement consisted in four unidirectional E-glass plies and the matrix was a dicyclopentadiene (DCPD) polyester resin. The coupon, with nominal dimensions of 450 × 400 × 3.23 mm, was produced by infusion and the fiber volume fraction was 58%. In-plane tensile properties of the coupon are listed in Table 2.

Specimens were cut using a diamond wheel cooled with ethyl alcohol and their dimensions were in agreement with ASTM

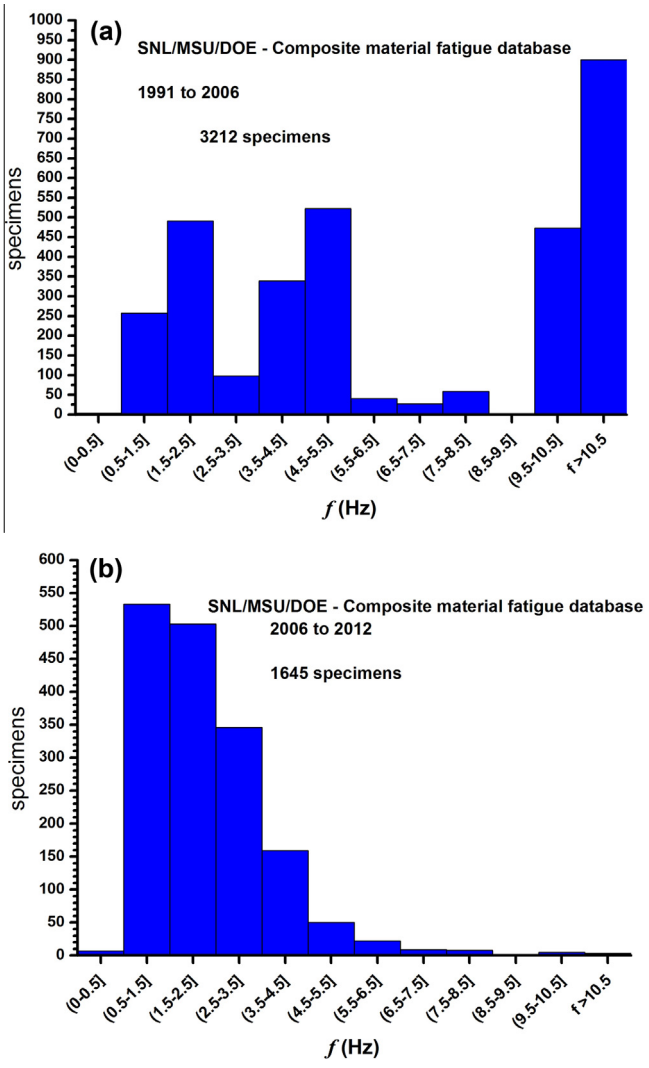

Fig. 1. Number of specimens of SNL/MSU/DOE database as a function of the loading frequency (a) from 1991 to 2006 and (b) from 2006 to 2012 [16].

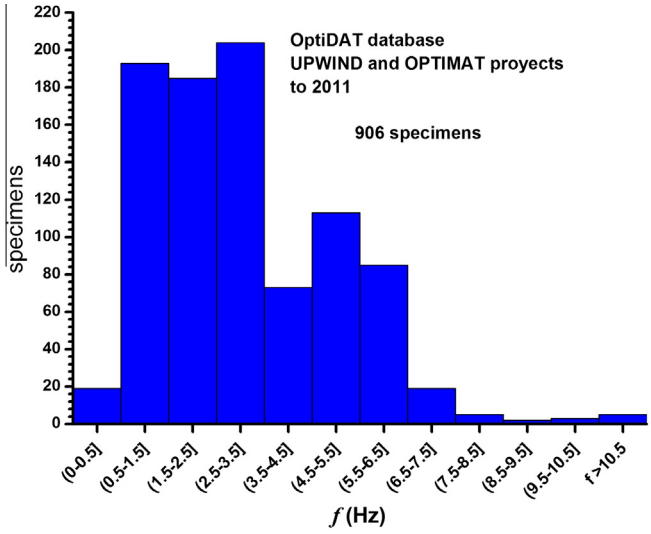

Fig. 2. Number of specimens of Knowledge Centre WMC database as a function of the loading frequency [17].

D2344 [20]. Five specimens were tested to determine quasi-static short-beam strength (F^{sbs}), employing a universal testing machine EMIC DL 2000. The fatigue machine, the test device and principal material directions are shown in Fig. 3. The fatigue machine performs fatigue tests under constant amplitude load cycles [21]. The force was measured with a load cell of 1.3 kN capacity and the displacement of the loading nose was measured with an LVDT Omega 500 (2.5 mm stroke). The SBS device was in accordance to requirements of ASTM D2344. A span-to-thickness ratio of 4.0 was adopted.

The SBS stress at *i*th data point corresponding to the neutral axis of the beam was calculated using Eq. (1). This equation assumes a parabolic stress distribution throughout the thickness, reaching its maximum value on the neutral axis of the beam [22].

$$\tau_{(i)}^{sbs} = \frac{3}{4}\frac{P_{(i)}}{bh} \tag{1}$$

The shear stress-ratio (R) was estimated according to Eq. (2) and shear stress amplitude (τ_a) with Eq. (3).

$$R = \frac{\tau_{\min}^{sbs}}{\tau_{\max}^{sbs}} \tag{2}$$

$$\tau_a = \frac{\tau_{\max}^{sbs} - \tau_{\min}^{sbs}}{2} \tag{3}$$

The stiffness loss of the specimen (δmax ratio) is defined in Eq. (4). The failure criterion adopted to stop the fatigue tests was a stiffness loss of 20% and all the specimens were carried out up to failure.

$$\delta\text{max ratio} = \frac{\delta\max_1}{\delta\max_N} \tag{4}$$

In some cases the variation in displacement at each load cycle to the variation in displacement at the first cycle ratio was measured (see Eq. (5)).

$$\Delta\delta \text{ ratio} = \frac{\delta\max_1 - \delta\min_1}{\delta\max_N - \delta\min_N} \tag{5}$$

Tests were conducted at a standard laboratory atmosphere (23 °C, 50%). The temperature of the specimen was monitored in the surface by means of a thermocouple; temperature changes below 1 °C were not considered. The tests were performed with a sinusoidal waveform at $R = 0.1$ and τ_a of 11.0, 13.2 and 15.7 MPa. τ_a values were selected based in previous experiences [23,24]. Between five to six specimens were tested for τ_a of 11.0 and 13.2 MPa and ten for 15.7 MPa. The loading frequencies were 1, 3, 6 and 10 Hz.

A single-factor analysis of variance was used to evaluate equality between mean values. The analysis was performed through the variance-stabilizing transformation of Eq. (6) and assuming a significance level (α) of 0.05 [25].

$$y_{ij}^{*} = \log N_{f_{ij}} \tag{6}$$

j is the observation in the treatment i.

Fitted curves were plotted together with the fatigue data. They have the form

$$\tau_a = \tau_0 N^{-\frac{1}{k}} \tag{7}$$

Table 1
Frequencies employed in apparent interlaminar shear fatigue tests.

Authors	Year	Composite material		Test	f (Hz)
		Fiber	Matrix		
Green and Pratt [5]	1975	Carbon	Epoxy	SBS	60
Bevan [11]	1977	Carbon	Epoxy	SBS	6.6
Phillips and Scott [6]	1977	Carbon, Kevlar, Glass	Epoxy	Torsion	0.17
Shokrieh and Lessard [7]	1998	Carbon	Epoxy	Double-Notch Shear	1–10
Degallaix et al. [8]	2002	Glass	Epoxy	Cube	10
Roudet et al. [12]	2002	Glass	Epoxy	SBS	10
Schaaf et al. [19]	2007	Glass	Epoxy	SBS	10
Makeev [13]	2013	Glass, Carbon	Epoxy	SBS	5

Table 2
In-plane tensile properties of the coupon.

Standard ASTM D3039-14	0° fiber direction			90° fiber direction		
	F^{tu} (MPa)	E^{chord} (GPa)	v	F^{tu} (MPa)	E^{chord} (GPa)	v
Mean	895	46.9	0.243	56.8	15.8	0.114
S	8	1.0	0.063	4.7	1.0	0.014
CV (%)	0.9	2.1	25.9	8.3	6.2	11.9

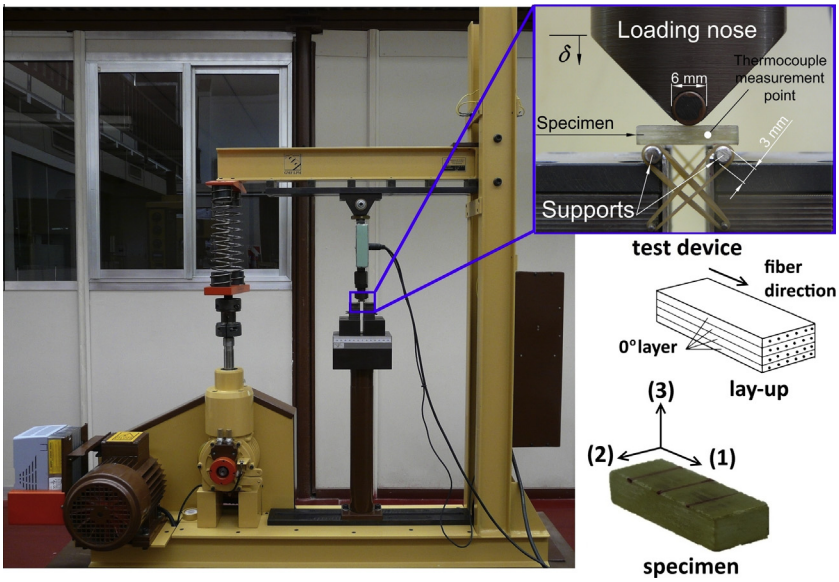

Fig. 3. Testing machine, test device and principal material directions.

Table 3
Results of quasi-static SBS tests.

Specimen	F^{sbs} (MPa)	Specimen	F^{sbs} (MPa)
CF 1	49.1	CF 4	48.6
CF 2	49.0	CF 5	49.0
CF 3	49.3		
Mean (MPa)	49.0	*CV* (%)	0.53
S (MPa)	0.3		

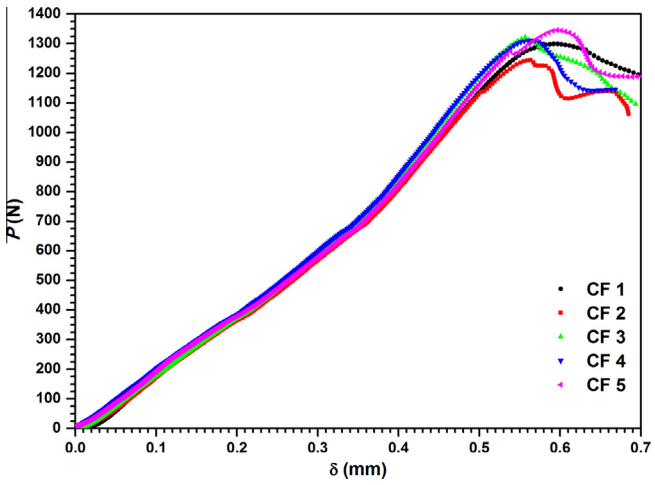

Fig. 4. Force–displacement curves of quasi-static SBS tests.

where τ_0 and k are fitting coefficients.

A Bartlett's test and a graphic of residuals versus fitted values were performed to verify that the residuals were structureless [25].

3. Results

The F^{sbs} results obtained from the quasi-static tests, including the values of sample mean, sample standard deviation (S) and sample coefficient of variation (CV) are presented in Table 3. The force–displacement curves of each specimen are shown in Fig. 4.

Table 4
SBS fatigue life at different shear stress amplitudes and frequencies.

1 Hz	3 Hz	6 Hz	10 Hz
τ_a = 15.7 MPa			
3880	9160	5820	12,820
4040	20,180	17,020	20,470
5430	4010	12,480	3060
7630	18,010	15,940	11,610
7860	29,050	2710	25,670
9620	1970	4760	4750
24,660	11,750	23,260	3600
4450	3860	8440	7600
8680	2590	4710	10,890
11,110	21,860	5510	16,820
τ_a = 11.0 MPa			
201,480	1,690,060	1,150,860	2,213,570
319,440	1,740,210	5,794,280	1,337,710
385,430	2,195,410	753,330	5,014,390
1,721,130	236,680	577,610	1,873,500
305,290	310,450	2,797,220	912,400
	3,419,910		
τ_a = 13.2 MPa			
190,870	326,970	54,590	278,990
235,400	57,320	64,950	324,710
95,500	111,110	70,620	104,880
39,420	123,060	80,280	19,870
232,670	419,790	103,790	178,170
355,570	231,770	157,700	176,650

SBS fatigue life results for different frequencies and shear stress amplitudes are presented in Table 4. These data are presented in τ_a as a function of log N_f graphs in Fig. 5a and b. A log-normal distribution was assumed to evaluate statistically these results (see Eq. (6)). The darkened points correspond to the calculated mean fatigue life values. Fig. 5b also shows the aforementioned fitted curves (Eq. (7)) for each frequency, together their corresponding coefficients of determination.

The logarithm of SBS fatigue life as a function of the loading frequency is shown in Fig. 6. The darkened points show the mean values.

The 1–3 material plane of a specimen before testing is shown in Fig. 7a and the same plane for a specimen after testing is shown in Fig. 7b. The tested specimens showed a typical interlaminar failure for all stress levels. Damage due to supports and the loading nose

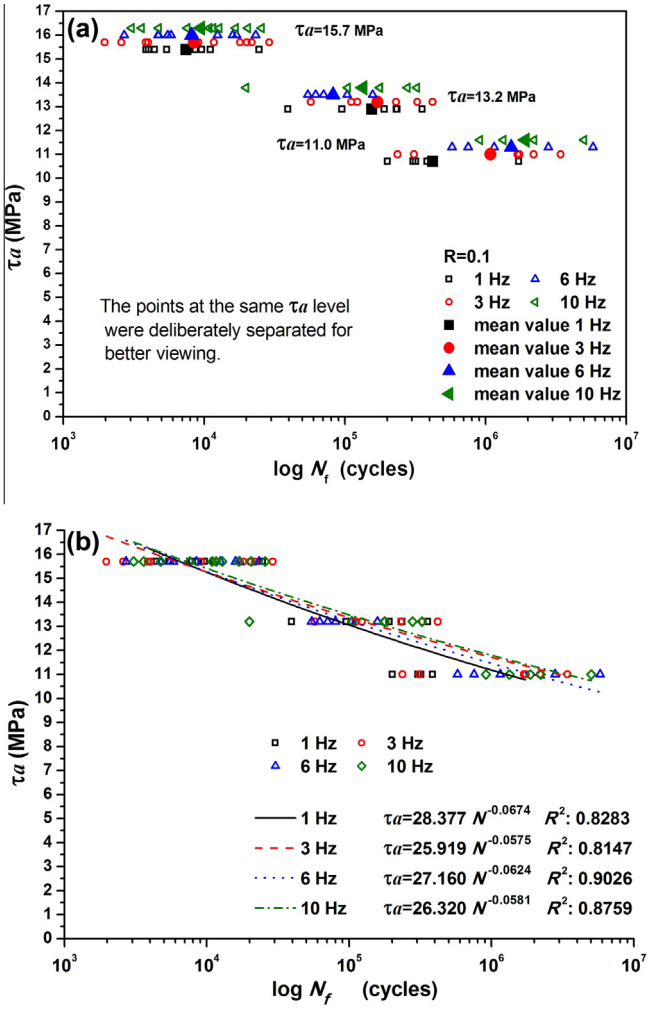

Fig. 5. Shear stress amplitude as a function of logarithm of SBS fatigue life for different frequencies.

were also present in all specimens. The damaged zone is observed as whitish zones in the specimens associated to changes in translucency. Interlaminar shear damage was observed either in one or both sides of the region between the loading nose and the supports.

Specimens with τ_a = 15.7 MPa and frequencies of 1 and 3 Hz presented a temperature increase in the surface up to 1 °C, while for 6 and 10 Hz the specimens showed temperature increases up to 4 °C and 7 °C respectively. The temperature increases in terms of the life ratio (cycles(N)/cycles to failure (N_f)) [1] for τ_a = 15.7 MPa at 6 and 10 Hz are shown in Fig. 8a. This increase of temperature also was observed for τ_a = 13.2 MPa at10 Hz as can be seen in Fig. 8b. The changes of temperature were unnoticed in specimens with τ_a = 13.2 MPa at 1, 3 and 6 Hz and τ_a = 11.0 MPa at all frequencies tested.

The stiffness change of a specimen at τ_a = 15.7 MPa and 1 Hz during the test is shown in Fig. 9a and b. The circles are values of δmax ratio and the triangles are values of $\Delta\delta$ ratio. In this specimen the test was continued after exceeding the failure criterion. This region is shown with angled lines. Fig. 9b shows the first 5% of the fatigue life of the specimen.

Bartlett's test results are shown in Table 5. The true hypothesis assumes that the four variances are the same. The analysis of variance results for the three stress amplitude values are presented in Tables 6–8.

4. Discussion

The study of the loading frequency effect in interlaminar shear stress fatigue is of particular interest in laboratory practice to be able to test specimens at the highest frequency without affecting the fatigue life. Moreover, it is also important to compare either experimental results performed with different frequencies or experimental results obtained with a frequency different to that of the structural component.

The SBS test is considered adequate in quasi-static loading for quality control and to compare materials under interlaminar shear stress conditions. Although it does not produce a uniform shear stress state [26,27], this simple test resulted appropriate to perform predominant interlaminar shear tests and was adopted by ASTM and ISO [20,28]. As in the case of quasi-static test, this test may be adequate in fatigue testing to compare materials and quality control under predominant interlaminar shear stress conditions. This test was chosen in this work and results were encouraging because visual inspection showed that all specimens presented interlaminar shear damage mode. Additionally, the change in the translucency of the specimens made possible to observe in more detail the damage in the thickness direction. The interlaminar damage of a tested specimen can be observed in the right side of Fig. 7b. Damaged zones due the loading nose and

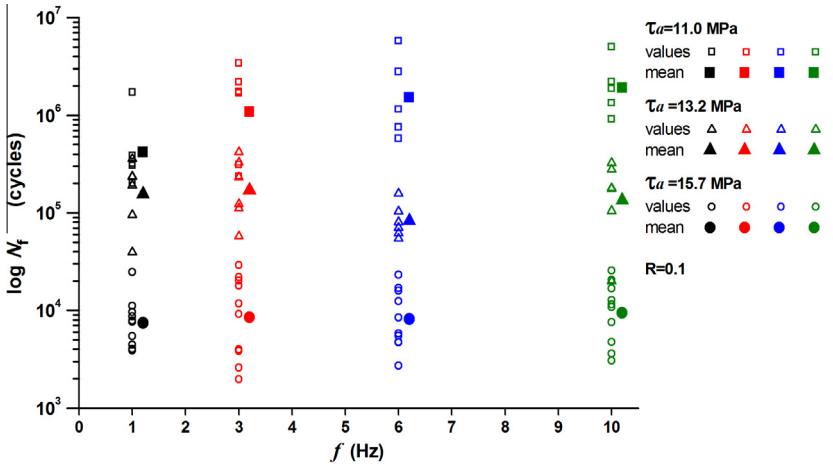

Fig. 6. Logarithm of SBS fatigue life as a function of loading frequency.

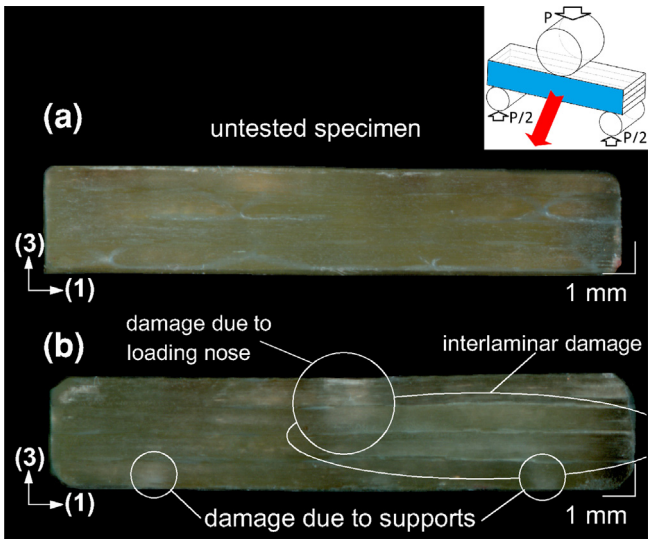

Fig. 7. (a) Untested specimen and (b) typical damage observed in the specimens.

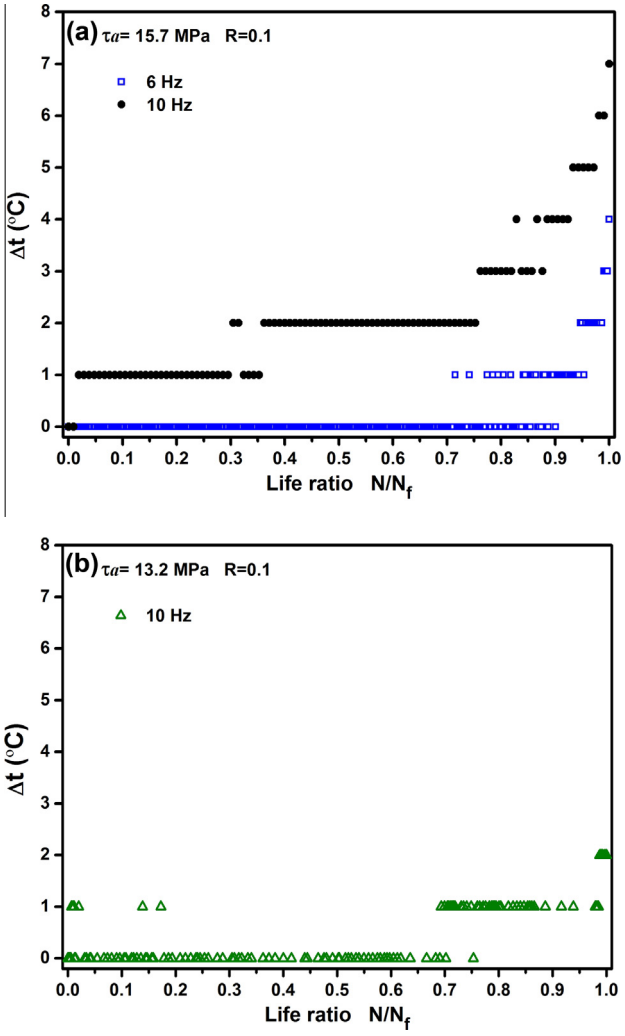

Fig. 8. Temperature increase as a function of normalized fatigue life.

the supports can be observed on the upper zone and on the bottom zone of the specimen respectively. The visual inspection of the specimens did not show differences in the damaged region between the three stress levels for all the employed frequencies. Instead, results in carbon reinforced epoxy obtained by May and Hallett [9] indicated that the damaged regions under the roller supports were smaller at reduced applied stress. These differences may be associated to the material, the failure criterion, the stress level or the geometry.

The range of frequencies evaluated in this paper (1–10 Hz) covers the most employed values in SNL/MSU/DOE and Knowledge Centre WMC databases (see Figs. 1 and 2) [16,17]. τ_a values were selected because they were expected to provide fatigue lives between 10^3 and 10^6 cycles based on previous results [23,24]. This range is typically employed in the characterization of high-cycle fatigue tests of composites and it corresponded approximately to results obtained experimentally. The quasi-static SBS tests results shown in Fig. 4 and Table 3 presented a F^{sbs} mean value according to similar materials [31] and a small value of standard deviation. Furthermore, load–displacement records showed similar behavior.

Results of fatigue tests shown in Fig. 5 were fitted with a model of the form of Eq. (7). All coefficient of determination were greater than 0.80. These values are not very high but are similar to results of fatigue if glass reinforced polymer [16,17]. The mean values of SBS fatigue life could not be compared with the obtained in other studies because no results of equivalent materials were found by the authors. Scatter was similar to the obtained in other studies performed with composites of glass fiber reinforced epoxy [12] and carbon fiber reinforced epoxy [9]. Results in Figs. 5 and 6 indicate differences in the fatigue life mean values for $\tau_a = 11.0$ MPa, being lower at lower frequencies. For $\tau_a = 13.2$ MPa at 6 Hz a slightly decrease on the fatigue life was observed. Sun and Chan [32] observed similar response but for $[\pm 45]_{2S}$ in tension fatigue of glass fiber reinforced epoxy. Instead, Figs. 5 and 6 do not show difference in the mean fatigue life values for an amplitude of $\tau_a = 15.7$ MPa.

The variance analysis was performed assuming a significance level α of 0.05 because it is one of the most commonly used [30,33,34]. Plots of normal probability as a function of residuals (not shown in this paper) have the look of straight lines. This implies that the normality assumption of the transformed populations may be adequate in both cases. The Bartlett's test in Table 5 reveals that the null hypothesis cannot be rejected; the four variances in both cases are the same. The variance analysis in Tables 6 and 7 indicates that the differences are not significant for a significance level α of 0.05. In the case of $\tau_a = 15.7$ MPa in Table 6, $F_0 < F_{0.05,3,36}$. Therefore, the null hypothesis (H_0: no difference in treatment means) should not be rejected. Alternatively, the P-value approach shows that $P = 0.914$. The null hypothesis would be rejected at a significance level >0.914. In the same way, the case of $\tau_a = 13.2$ MPa in Table 7, $F_0 < F_{0.05,3,20}$ and $\alpha < P$-value = 0.389. The null hypothesis should not be rejected.

The case of $\tau_a = 11.0$ MPa in Table 8 is more complicated. As in the previous case, $F_0 < F_{0.05,3,17}$ and P-value = 0.08 is greater than the adopted α value. This implies that the null hypothesis should not be rejected. However, the differences are smaller than in the other two τ_a levels. The P-value approach for this case shows that P-value is close to the significance level adopted. The statistical analysis indicated that the differences between mean lives at different frequencies resulted not significant for the studied conditions.

As already mentioned, the temperature variation during the fatigue tests was recorded. The measurement was performed in the zone where the interlaminar stresses are maximum (see Fig. 3) and where fatigue damage initiation is prone to nucleate. Because of the measurement is superficial and localized, it is not discarded that the temperature may be higher inside the specimen. Other important temperature variations may be produced by the complex stress–strain state in the specimen that may produce

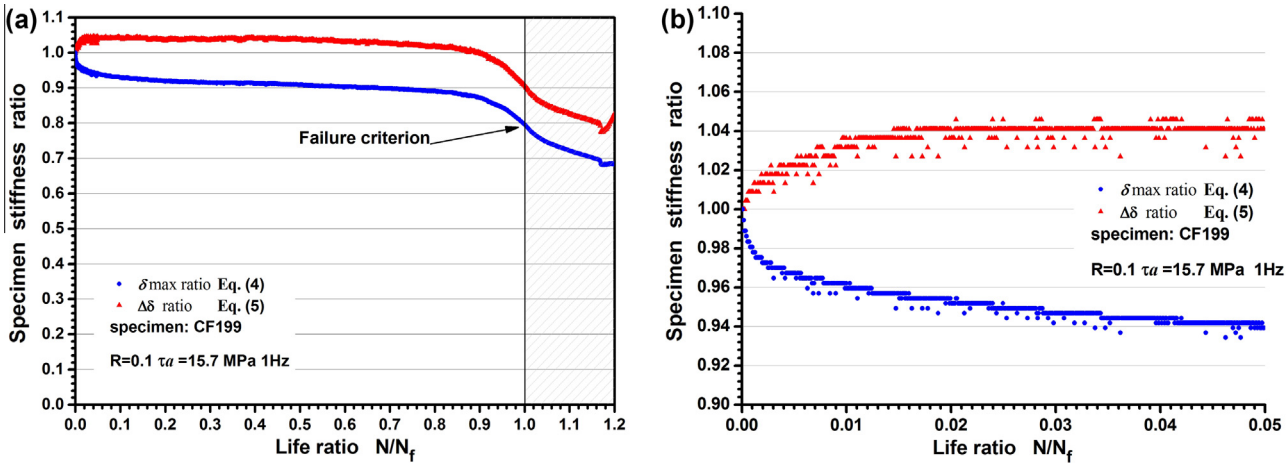

Fig. 9. Specimen stiffness ratio as a function of normalized fatigue life.

temperature gradients. Khan and Muliana [35] modeled a short-beam of particle-reinforced composite under cyclic bending. Their model considerers isotropic homogeneous material, uniformly distributed load and $R = -1$. The largest temperature increment in the model occurred in the outer faces of the middle of span. This research differs from their model mainly because long fiber orthotropic material was employed and concentrated instead of uniformly distributed load was applied. The temperature measurements obtained in this paper can be used to compare temperatures corresponding to different experimental situations. Specimens with $\tau_a = 15.7$ MPa at 6 and 10 Hz, and $\tau_a = 13.2$ MPa at 10 Hz showed the largest temperature increases. The temperature increment was continuous, being noticeable in the last 30% of the fatigue life as can be observed in Fig. 8a and b. In case another failure criterion is adopted, for example another value of stiffness reduction, the maximum temperature increase might be different. The temperature changes in specimens with $\tau_a = 15.7$ MPa at 1 or 3 Hz was small, about 1 °C. ASTM D3479 [36] for tension–tension fatigue testing of composite laminates makes a recommendation of caution referred to the frequency selection due to specimen temperature variation. This standard says that degradation of material properties was observed in some composites with a temperature increase of 10 °C. ISO 13003 [2] limits the self-generated heating to 10 °C temperature rise. In the test conditions employed in this study, the temperature increases were up to 7 °C. The tests corresponding to $\tau_a = 15.7$ MPa and of $\tau_a = 13.2$ MPa at 10 Hz showed differences in the specimen heating. Nevertheless, the statistical analysis of the results showed that there is not a

Table 5
Results of the Bartlett's test for different τ_a levels.

$H_0: \ \sigma_1^2 = \sigma_2^2 = \sigma_3^2 = \sigma_4^2$		
H_1: above not true for at least one		
$\alpha = 0.05$	$\chi^2_{0.05,3}$	7.81
$\tau_a = 11.0$ MPa	χ^2_0	1.22
$\tau_a = 13.2$ MPa	χ^2_0	3.79
$\tau_a = 15.7$ MPa	χ^2_0	2.71

Table 6
Analysis of variance for fatigue life with $\tau_a = 15.7$ MPa.

Source of variations	Sum of squares	Degrees of freedom	Mean square	F_0	P-value	$F_{0.05,3,36}$
f	0.0558	3	0.0186	0.1727	0.914	2.866
Error	3.8785	36	0.1077			
Total	3.9343	39				

Table 7
Analysis of variance for fatigue life with $\tau_a = 13.2$ MPa.

Source of variations	Sum of squares	Degrees of freedom	Mean square	F_0	P-value	$F_{0.05,3,20}$
f	0.3563	3	0.1187	1.056	0.389	3.098
Error	2.2484	20	0.1124			
Total	2.6047	23				

Table 8
Analysis of variance for fatigue life with $\tau_a = 11.0$ MPa.

Source of variations	Sum of squares	Degrees of freedom	Mean square	F_0	P-value	$F_{0.05,3,17}$
f	1.2584	3	0.4195	2.676	0.080	3.197
Error	2.6645	17	0.1567			
Total	3.9229	20				

significant difference between the means. For τ_a = 11.0 MPa, the self-generated heating was unnoticed and results at different frequencies showed more differences in mean lives, although they were not significant. Nevertheless, as discussed above, the significance level was close to the *P*-value. In this stress level, the effect of rate dependence may be more import than the heating effect [1,2].

At the highest stress level, where large temperature increments were observed, the differences between mean lives corresponding to the studied frequencies resulted very small and clearly not significant. Instead, at the lowest stress level, where the temperature increments were not noticed, the difference between means was not significant but close to be significant. The general trend is that the mean life is large for large frequencies, though at intermediate frequencies this tendency is the opposite, more clearly for τ_a = 13.2 MPa. This apparent contradiction may be originated by the limited test data or it may be consequence of a rate dependence effect. As discussed above, Sun and Chan [32] observed a similar response for $[\pm 45]_{2S}$ in tension–tension fatigue of glass fiber reinforced epoxy.

The specimen stiffness change as failure criterion [12,29,30] was easy, practical and adequate to be implemented in this study. Three regions in the specimen stiffness degradation curve (δmax ratio) can be observed in Fig. 9a. The third region, where the specimen shows a sudden δmax ratio degradation, also is observed for $\Delta\delta$ ratio. However, in the case of $\Delta\delta$ ratio an apparent increase in the specimen stiffness was observed. This covers approximately the first 90% of the fatigue life. May and Hallett [9] suggested that this may be caused by load redistribution due to damage initiated in a region of combined compressive and shear stresses and localized wear under the supports. Fig. 9b shows the first 5% of the fatigue life where this phenomenon is better appreciated: 4% increase of $\Delta\delta$ ratio and 6% decrease of δmax ratio. Daniels et al. [37] observed important stiffness changes in quasi-static loaded SBS specimens at temperatures approaching the glass transition temperature. Instead, their results show that small temperature increases did not produce important changes in the specimen stiffness when the temperature was below the glass transition temperature. No differences were observed in this study in the specimen stiffness ratio vs. the life ratio curves for τ_a = 15.7 MPa. Nevertheless, it may be important for variations in material (other fiber and/or matrix, fiber volume fraction, rate temperature dependence) or in test conditions (*R*-values, frequencies).

In this paper *R* = 0.1 was used because it was one of the most frequently employed loading ratios in interlaminar shear fatigue studies [4,7–9,13]. Other *R*-values may be required to characterize the SBS fatigue behavior in order to obtain a constant life diagrams (CLD) by interlaminar shear. The mean stress effect in combination with the loading frequency effect might have influence in interlaminar shear fatigue life, reason why this combined effect is under study as a continuation of this research.

The specimen dimension is another variable that may affect the SBS fatigue life. The dimensions in quasi-static SBS test given by the standards are proportional to the thickness. This produces variations in the area-to-volume ratio that may change the heat transfer rate to the environment. Differences should be noted whether standardized quasi-static SBS specimen dimensions were employed. ASTM D2344 [20] limits the thickness (h) between 2 and 6 mm but ISO 14130 [28] does not limit this geometric value. The extreme values of area-to-volume ratios for ASTM D2344 are 1.67 and 0.56. This implies that a specimen with h = 2 mm presents a value of area-to-volume ratio 3 times larger than a specimen with h = 6 mm. The SBS fatigue tests reported in literature used several width-to-thickness ratios (b/h), length-to-thickness ratio (l/h) and area-to-volume values. Makeev [13] used a b/h = 0.8 and an area-to-volume ratio of 0.83. This author argues that b/h values approximately 1 produce a strain distribution through the specimen width more uniform than the suggested value of 2.0 in ASTM D2344. May and Hallett [9] used a b/h = 3.9 and an area-to-volume ratio of 1.07. Bevan [11] used a b/h = 5 and an area-to-volume ratio of 1.04. In this study a b/h = 2.0 and an area-to-volume ratio of 1.03 were used. This variation should be analyzed and taken into account if the test is going to be standardized for fatigue tests.

5. Conclusions

SBS tests were performed in quasi-static and fatigue conditions. This test showed simplicity to perform predominant interlaminar shear fatigue test.

All the specimens presented interlaminar shear damage around the neutral axis and localized damage near the loading nose and the supports.

Specimens with the smallest shear stress amplitude showed a fatigue life between 10^5 and 10^6 cycles and the temperature rise was unnoticed. Specimens with the highest shear stress amplitude endured approximately 10^4 cycles and their temperature rises were up to 7 °C at 10 Hz, 4 °C at 6 Hz and 1 °C at both 1 and 3 Hz.

The frequency sensitivity was large at low stress amplitude, although the statistical analysis of the results indicated that the differences in mean values resulted not significant in the studied conditions.

Acknowledgments

The authors wish to thanks CONICET and IMPSA for the scholarship of Héctor G. Kotik. The authors also thank to Eduardo Benotti (GMF-LPM) for his invaluable aid in the construction of the test devices. This research was supported by IMPSA and CONICET [RD20120523-1548].

References

[1] Vassilopoulos AP. Fatigue life prediction of composites and composite structures. 1st ed. Boca Raton: CRC Press; 2010.
[2] Sims GD. Fatigue test methods, problems and standards. In: Harris B, editor. Fatigue in composites. Boca Raton: CRC Press; 2003. p. 36–62.
[3] Nijssen RPL. Phenomenological fatigue analysis and life modelling. In: Vassilopoulos AP, editor. Fatigue life prediction of composites and composite structures. Boca Raton: CRC Press; 2010. p. 47–101.
[4] Pipes RB. Interlaminar shear fatigue characteristics of fiber-reinforced composite materials. In: Berg CA, McGarry FJ, Elliott SY, editors. ASTM STP 546 composite materials: testing and design. Williamsburg: ASTM international; 1974. p. 419–32.
[5] Green AK, Pratt PL. The shear fatigue behaviour of a unidirectional cfrp. Composites 1975;6:246–8. http://dx.doi.org/10.1016/0010-4361(75)90009-9.
[6] Philllips DC, Scott JM. The shear fatigue of unidirectional fibre composites. Composites 1977;8:233–6. http://dx.doi.org/10.1016/0010-4361(77)90108-2.
[7] Shokrieh MM, Lessard LB. An assessment of the double-notch shear test for interlaminar shear characterization of a unidirectional graphite/epoxy under static and fatigue loading. Appl Compos Mater 1998;5:49–64. http://dx.doi.org/10.1023/A:1008866705868.
[8] Degallaix G, Hassaïni D, Vittecoq E. Cyclic shearing behaviour of a unidirectional glass/epoxy composite. Int J Fatigue 2002;24:319–26. http://dx.doi.org/10.1016/S0142-1123(01)00087-1.
[9] May M, Hallett SR. An assessment of through-thickness shear tests for initiation of fatigue failure. Compos A: Appl Sci Manuf 2010;41:1570–8. http://dx.doi.org/10.1016/j.compositesa.2010.07.005.
[10] Carlsson L, Adams DF, Byron PipesR. Experimental characterization of advanced composite materials. 3rd ed. Boca Raton: CRC Press LLC; 2003.
[11] Bevan LG. Axial and short beam shear fatigue properties of cfrp laminates. Composites 1977;8:227–32. http://dx.doi.org/10.1016/0010-4361(77)90107-0.
[12] Roudet F, Desplanques Y, Degallaix S. Fatigue of glass/epoxy composite in three-point-bending with predominant shearing. Int J Fatigue 2002;24:327–37. http://dx.doi.org/10.1016/S0142-1123(01)00088-3.
[13] Makeev A. Interlaminar shear fatigue behavior of glass/epoxy and carbon/epoxy composites. Compos Sci Technol 2013;80:93–100. http://dx.doi.org/10.1016/j.compscitech.2013.03.013.
[14] ASTM International. ASTM WK34935 new practice for short beam fatigue response of polymer matrix composite materials and their laminates. <http://www.astm.org/DATABASE.CART/WORKITEMS/WK34935.htm> [access date 24/04/2015].

[15] Harris B. Fatigue in composites: science and technology of the fatigue response of fibre-reinforced plastics. Boca Raton: CRC Press; 2003.
[16] Sandia National Labs, Montana State University. Blade materials & structures testing database. <http://energy.sandia.gov/energy/renewable-energy/wind-power/wind-software-downloads/wind-and-water-materials-and-structures-database/> [access date: 24/02/13].
[17] Knowledge Centre WMC, Optidat Database. <http://www.wmc.eu/optimatblades_optidat.php> [access date: 30/04/2015].
[18] Van Wingerde A, Van Delft D, Janssen L, Philippidis TP, Brøndsted P, Dutton A, et al. OPTIMAT BLADES: results and perspectives. In: Scientific proceedings of the European wind energy conference and exhibition. p. 69–72.
[19] Schaaf K, Rye P, Nemat-Nasser S. Optimization studies of self-sensing composites. In: The 14th international symposium on: smart structures and materials & nondestructive evaluation and health monitoring. International Society for Optics and Photonics; 2007. p. 65292X. http://dx.doi.org/10.1117/12.716091.
[20] ASTM D 2344/D 2344M-13. Standard test method for short-beam strength of polymer matrix composite materials and their laminates. West Conshohocken (PA): ASTM International; 2013. http://dx.doi.org/10.1520/D2344_D2344M.
[21] Pach E, Korin I, Ipina J. Simple fatigue testing machine for fiber-reinforced polymer composite. Exp Tech 2012;36:76–82. http://dx.doi.org/10.1111/j.1747-1567.2011.00713.x.
[22] Timoshenko S, Timoshenko S, Goodier J. Theory of elasticity. McGraw-Hill Book Company; 1951.
[23] Kotik H, Ipiña J Perez. Influence of Unifilo® Ply in the interlaminar shear fatigue resistance of GFRP. Proc Mater Sci 2015;8:139–47. http://dx.doi.org/10.1016/j.mspro.2015.04.057.
[24] Kotik H, Perez Ipiña J. Frequency effect in short-beam fatigue of GFRP. In: COMAT 2015 6th international conference on science and technology of composite materials, Buenos Aires; 2015. p. P2.4
[25] Montgomery DC. Design and analysis of experiments. 7th ed. Hoboken: Wiley; 2008.
[26] Whitney J, Browning C. On short-beam shear tests for composite materials. Exp Mech 1985;25:294–300. http://dx.doi.org/10.1007/BF02325100.
[27] Makeev A, He Y, Schreier H. Short-beam shear method for assessment of stress–strain curves for fibre-reinforced polymer matrix composite materials. Strain 2013;49:440–50. http://dx.doi.org/10.1111/str.12050.
[28] ISO 14130-1998. Fiber-reinforced plastic composites-determination of apparent interlaminar shear strength by short beam method. ISO international; 1998.
[29] Salkind M. Fatigue of composites. In: Corten HT, editor. ASTM STP 497 composite materials testing and design (2nd Conf). West Conshohocken: ASTM International; 1972. p. 143–69.
[30] Vassilopoulos AP, Keller T. Fatigue of fiber-reinforced composites. London: Springer; 2011.
[31] Kotik H, Appiolaza G, Tumbarello S, Perez Ipiña J. Comparación de propiedades mecáncias de materiales compuestos de matriz poliéster ortoftálica y poliéster DCPD. In: CONAMET/SAM 2012. 12° Congreso Binacional de Metalurgia y Materiales, Valparaíso; 2012. p. 164.
[32] Sun C, Chan W. Frequency effect on the fatigue life of a laminated composite. In: Tsai SW, editor. ASTM STP 674 Composite materials: testing and design (fifth conference). New Orleans: ASTM International; 1979. p. 418–30.
[33] ASTM E 739-91. Standard practice for statistical analysis of linear or linearized stress–life (S–N) and strain–life (ε–N) fatigue data. West Conshohocken (PA): ASTM International; 2004. http://dx.doi.org/10.1520/E0739-91R04.
[34] Young L, Ekvall J. Reliability of fatigue testing. In: Little RE, Ekvall JC, editors. ASTM STP 744 statistical analysis of fatigue data. Pittsburgh: ASTM International; 1981. p. 55–74.
[35] Khan KA, Muliana AH. Fully coupled heat conduction and deformation analyses of nonlinear viscoelastic composites. Compos Struct 2012;94:2025–37. http://dx.doi.org/10.1016/j.compstruct.2012.01.010.
[36] ASTM D 3479/D3479M-12. Standard test method for tension–tension fatigue of polymer matrix composite materials. West Conshohocken: ASTM International; 2012. http://dx.doi.org/10.1520/D3479_D3479M-12.
[37] Daniels BK, Harakas NK, Jackson RC. Short beam shear tests of graphite fiber composites. Fibre Sci Technol 1971;3:187–208. http://dx.doi.org/10.1016/0015-0568(71)90002-9.